Chapter 11

Carbon Nanotube Composites as Electromagnetic Shielding Materials in GHz Range

Marta González, Guillermo Mokry, María de Nicolás, Juan Baselga and Javier Pozuelo

Additional information is available at the end of the chapter

http://dx.doi.org/10.5772/62508

Abstract

Following the development of the new electronic systems and communication networks, the levels of electromagnetic contamination have risen dramatically in the recent years. Every day, new studies appear searching for a way to mitigate the electromagnetic interferences (EMI). At the same time, the rapid evolution of technology forces the field to search for lighter and more efficient materials. The composites using carbon allotropes (such as carbon nanotubes) and polymers as reinforcement are gaining importance, due to the many advantages they exhibit in comparison to the materials that were used until now. A great number of applications require absorption to be the main electromagnetic shielding mechanism, thereby making this review necessary as a way to summarize the latest studies on CNT/polymer composites and how to improve the absorption mechanism by changing the morphology and composition of CNTs.

Keywords: Carbon nanotube, Electromagnetic shielding materials, Electromagnetic characterization, Nanocomposite, Electromagnetic absorber

1. Introduction

Electromagnetic interferences (EMIs) occur when electromagnetic signals are unintentionally transmitted from an emitter to another element by radiation and/or conduction, causing it to behave in an unexpected way [1]. The problem arises from high-frequency signals coupled to the main one that will radiate as they are conducted through and along the power wire. The wire will behave as an antenna that will pick up other signals and transfer them to the circuit

elements of the device [2]. EMIs, though part of our modern world, affect all electrical and electronic devices, which are more indispensable everyday for the society. EMI shielding is thus needed to suppress or attenuate electromagnetic radiation from emitters with materials that are able to interact with those signals. Thus, one of the present needs is to find broad-band shields, able to neutralize electromagnetic radiation in the GHz range. This requirement arises from the fast development of electronics, which has led to microprocessors with greatly enhanced data transfer speeds that operate at higher frequencies. Furthermore, the miniaturization and manufacturing of such components demand high-performance and lightweight materials. Due to the wide impact of telecommunications, several financially strong industrial sectors are expectant about the progress of EMI shielding materials. These technological fields demand not only efficient shields but also materials that meet specific criteria for each engineered design. For example, chemical and corrosion resistance, lightweight, flexibility, tuneable morphology, processing easiness and inexpensiveness are requirements that the materials must fulfil in order to be applicable in flexible electronics (e.g., personal computers and mobile phones), aerospace (e.g., satellite and aircraft´s manufacture) and automotive (e.g., integrated circuits) industries [3]. In the field of aerospace engineering, a challenging sector is focused on military stealth. For this specific purpose, radar-absorbing materials are needed. Much effort has been done in this direction although absorption of electromagnetic energy remains challenging, due to the need of accomplishing both low-reflection and high-absorption losses [2].

The exploration of new functional materials that enable to effectively block or filter broad-band electromagnetic energy is an active field of research nowadays. Polymers offer several advantages over traditional metals and ceramics used for EMI shielding. They can be easily shaped; it is possible to prepare a variety of configurations and formulations and they are substantially lighter. Although polymers are electromagnetically transparent, different strategies are available to convert them into active electromagnetic shields. Graphite, carbon black and carbon fibres were the first to be combined with polymers for the fabrication of EMI shields [3–5]. The attention soon shifted to nanocarbons, since with lower-weight fractions, more conductive composites could be obtained. In addition, to enable the entire cross-section of a filler to be active in shielding, the dimensions of the conductive filler should be less than the length of penetration of the incident radiation [6]. This penetration length is usually very small for good conductors at high frequencies. Thereby, nanocarbon fillers are adequate to shield in the GHz range. In this context, carbon nanofibres, nanotubes and graphene, which have higher specific surface area and aspect ratio than their microscale analogues, are promising candidates for the preparation of efficient EMI shielding composites. Despite having been studied extensively in recent years, several factors affecting the performance of nanocarbon/polymer composites as high-frequency electromagnetic shields remain unexplored or not completely understood up to date. Indeed, there are few reported reviews on this application of nanocarbons [7–10], which show the need for new and reproducible experimental data to facilitate the construction of realistic models to improve our understanding.

http://dx.doi.org/10.5772/62508

2. Electromagnetic shielding mechanism

When an electromagnetic wave (E_I) impacts on a material (**Figure 1**), two waves are created on the surface: a reflected wave (E_R) and a transmitted wave into the material (E_{I-R}). Inside the material, a fraction of the wave (E_{I-R}) may be dissipated as heat (E_A) until it reaches the second surface of the material. At this point, two new waves appear: one that is transmitted through the surface (E_T) and a new wave that is reflected into the material. This process is repeated successively until it meets the criteria stated in equation 1:

$$E_I = \sum E_R + \sum E_A + \sum E_T \tag{1}$$

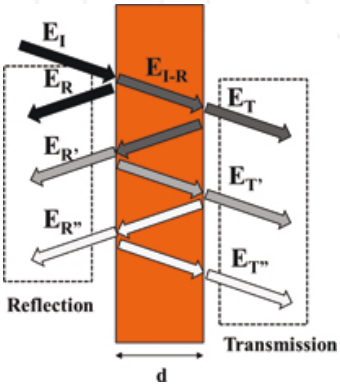

Figure 1. Mechanisms of attenuation of the incident EM power when it strikes a finite-dimensional media.

Both in the reflection and transmission processes, waves generated at each step may cause constructive and destructive interferences depending on the sample thickness and frequency. The reflection process on each plane of the material is what is called multiple reflections. Therefore, the electromagnetic shielding efficiency, *SE*, of a material can be quantified as the sum of three contributions: reflection, absorption and multiple reflections.

$$SE = SE_R + SE_A + SE_{MR} \tag{2}$$

The electromagnetic shielding efficiency can be expressed as a function of: impedance mismatch between the medium and the material (η_0 and η), sample thickness (d) and skin thickness (δ):

$$SE = 20log\left(\frac{\eta}{4\eta_0}\right) + 20log\left(exp\left(\frac{d}{\delta}\right)\right) + 20log\left(1 - exp\left(\frac{2d}{\delta}\right)\right) \tag{3}$$

where the skin thickness is defined as the depth at which the field decreases to 1/*e* from its initial value and is a function of frequency (*f*), permeability (μ) and conductivity (σ):

$$\delta = \left(\pi f \mu \sigma\right)^{-1/2} \tag{4}$$

The impedance can be expressed as the relation between the electric and the magnetic fields, where *j* accounts for an imaginary value and ε for the complex permittivity:

$$\eta = \frac{|E|}{|H|} = \left(\frac{j2\pi f \mu}{\sigma + j2\pi f \varepsilon}\right)^{1/2} \tag{5}$$

If the conductivity of the propagation medium is zero ($\sigma = 0$) and the conductivity in the conductive material is($\sigma \gg 2\pi f\varepsilon$), equation 5 can be simplified as:

$$\eta_0 = \left(\frac{\mu_0}{\varepsilon_0}\right)^{1/2} \quad and \quad \eta_0 = \left(\frac{2\pi f \mu}{\sigma}\right)^{1/2} \tag{6}$$

where the 0 index stands for the values in free space. Multiple reflections can be neglected when the sample thickness is bigger than the skin thickness. In this case, the absorbed radiation is high enough so that those constructive and destructive interferences cannot be produced, and only two mechanisms are possible in the electromagnetic shielding process: reflection and absorption. Taking this into account, and using equations 4 and 6, the electromagnetic shielding (equation 3) can be expressed as:

$$SE = \left[39.5 + 10log\left(\frac{\sigma}{2\pi f \mu}\right)\right] + \left[8.7d\left(\pi f \mu \sigma\right)^{1/2}\right] \tag{7}$$

Electromagnetic shielding can be determined from the reflection (*R*), absorption (*A*) and transmission (*T*) coefficients as a function of the reflected, transmitted and incident powers (P_R, P_T and P_I, respectively), and therefore:

$$R = \frac{P_R}{P_I}; T = \frac{P_T}{P_I}; A = 1 - \left(R + T\right) \tag{8}$$

In this way, the electromagnetic shielding can be expressed as:

http://dx.doi.org/10.5772/62508

$$SE = 10log\left(\frac{1}{T}\right); SE_R = 10log\left(\frac{1}{1-R}\right); SE_A = 10log\left(\frac{1-R}{T}\right); \quad (9)$$

3. Measurement techniques

With a "Network Analyser," it is possible to study the properties of electrical networks, especially those associated with reflection and transmission of electrical signals, known as scattering parameters, from a few MHz to 100 GHz. A two-ports network analyser emits electromagnetic radiation (*I*) in the required frequency range from each side, and analyses the reflected (*R*) and transmitted radiation (*T*) through the studied material. The three most common configurations for measuring solid samples are waveguide, coaxial line and free space arrangements (**Figure 2**).

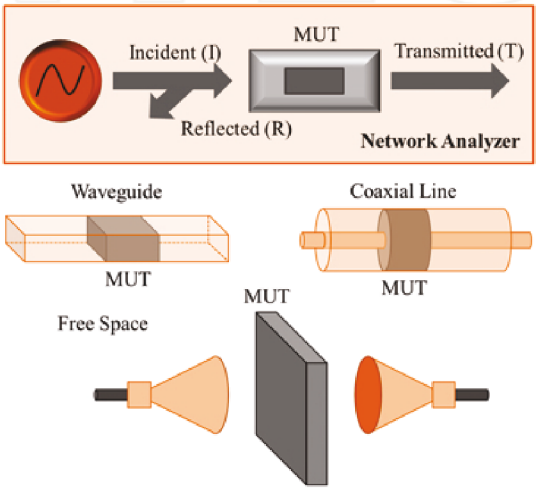

Figure 2. Configurations for EMI measuring solid samples.

Waveguide. Usually, it has a rectangular section. The sample is introduced at a precise distance from the waveguide end. The size of the waveguide depends on the frequency range for which it is prepared, and size decreases with increasing frequencies. The advantage of this system is the easiness of the sample preparation. The disadvantage is the narrow range of frequencies that can be measured. This causes that several waveguides are necessary to measure at high-frequency ranges.

Coaxial line. The sample is introduced between the inner and the outer conductors at an exact distance from the ends, and must be prepared as a rectangular toroid. For example, a coaxial line for measuring frequencies from 0.5 to 18 GHz has an inner conductor of 3.04 mm and a 7.00 mm external conductor. The main advantage is that it is possible to measure at high-frequency ranges on the same sample.

Free Space. It is a non-contact measurement based on two opposing antennae, flanking the sample. With this system, it is possible to measure a wide range of frequencies and to modify the angle of incidence of radiation on the samples. The most important disadvantage of this system is that the size of the samples must be considerably bigger than the previous techniques: Dimension range is from 30–40 cm for a few GHz to 10–15 cm for frequencies near 20 GHz.

With a two-ports network analyser, the voltage ratio between the generated and the returning electromagnetic waves for both ports is obtained (**Figure 3**).

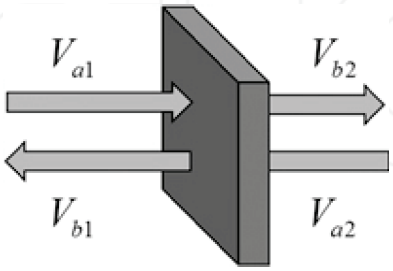

Figure 3. Voltage generated and returning in a two-ports network analyser.

where $V_{a1}\, yV_{a2}$ are voltages that come out of ports 1 and 2, respectively, and $V_{b1}\, yV_{b2}$ are voltages that return to ports 1 and 2, respectively. These voltages are related to the scattering parameters as:

$$\begin{pmatrix} V_{b1} \\ V_{b2} \end{pmatrix} = \begin{pmatrix} S_{11} & S_{12} \\ S_{21} & S_{22} \end{pmatrix} \begin{pmatrix} V_{a1} \\ V_{a2} \end{pmatrix} \tag{10}$$

Therefore,

$$V_{b1} = S_{11}V_{a1} + S_{12}V_{a2} \quad \text{and} \quad V_{b2} = S_{21}V_{a1} + S_{22}V_{a2} \tag{11}$$

According to the maximum transfer theorem, if the opposite port is charged with an identical voltage to the system impedance, then scattering parameters will be:

$$S_{11} = \frac{V_{b1}}{V_{a1}}; S_{22} = \frac{V_{b2}}{V_{a2}}; S_{12} = \frac{V_{b1}}{V_{a2}}; S_{21} = \frac{V_{b2}}{V_{a1}} \tag{12}$$

If the material is homogeneous, then $S_{11} = S_{22}$ and $S_{12} = S_{21}$. Therefore, S_{11} is the reflection produced in the sample and S_{21} is the transmission through the sample. The coefficients of reflection, absorption and transmission powers will therefore be expressed as:

http://dx.doi.org/10.5772/62508

$$R = \frac{P_R}{P_I} = |s_{11}|^2 \tag{13}$$

$$T = \frac{P_T}{P_I} = |s_{21}|^2 \tag{14}$$

$$A = 1 - (R - T) = 1 - \left(|S_{11}|^2 + |S_{21}|^2\right) \tag{15}$$

And therefore the shielding effectiveness is:

$$SE_T = 10log\left(\frac{1}{T}\right) = 10log\left(\frac{1}{|s_{21}|^2}\right) \tag{16}$$

$$SE_R = 10log\left(\frac{1}{1-R}\right) = 10log\left(\frac{1}{1-|s_{11}|^2}\right) \tag{17}$$

$$SE_A = 10log\left(\frac{1-R}{T}\right) = 10log\left(\frac{1-|s_{11}|^2}{|s_{21}|^2}\right) \tag{18}$$

Shielding effectiveness gives information about the preferred deactivation mechanism, while coefficients provide information on the fractions of the radiation lost by reflection and absorption, when multiple reflections are neglected. Multiple reflections produced by the interference of the reflected radiation in the first plane of incidence, and reflection produced in the last plane of the material, originate constructive and destructive interference dependant on the frequency. According to the Schelkunoff's theory [11–13], multiple reflections can be neglected when the sample thickness is larger than the skin depth, as mentioned above.

Figure 4 shows the skin depth as a function of frequency for samples with conductivities of 20, 30, 40 and 50 $S.m^{-1}$. In samples with a thickness of 4 mm, multiple reflections may be negligible above 5 GHz. In **Figure 4b**, the effect of multiple reflections on measurements of two different samples with the same thickness is shown. We can observe that the red sample gives a signal close to 2 GHz while the black sample gives three signals close to 2, 5 and 9 GHz, mainly due to the lower conductivity of the black sample. In order to avoid the sample

thickness causing misleading reflections due to multiple reflections, the minimum frequency for a shielding study must be 5 GHz for the sample in red and 11 GHz for the sample in black.

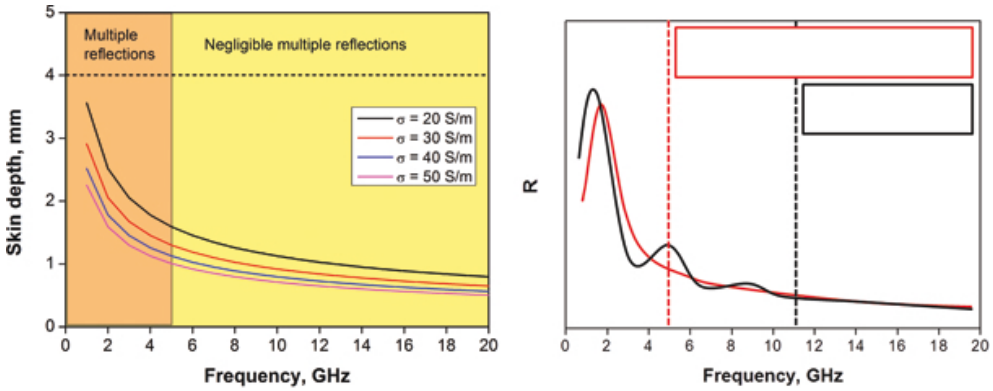

Figure 4. (a) Skin depth as a function of frequency for samples with different conductivities. (b) Effect of multiple reflections of two samples with the same thickness and different conductivity. Colored rectangles show the frequency range where multiple reflections are negligible.

4. Electrical properties of CNT composites

Electromagnetic shielding is closely related to the electrical properties of the composite. Although several conducting particles have been studied, such as carbon black particles [14], carbon fibres [15] or metallic fillers [16], CNTs have clearly demonstrated better properties due to their high aspect ratio (L/d), higher strength and flexibility and lower density, making them ideal as fillers.

There is a point, depending on the filler concentration in the composite, at which a conductive path is formed. This point has also been defined as the least concentration at which a composite with conductive inclusions is capable of conducting direct current. This is known as "percolation threshold," the point at which conductivity increases greatly. Although a broad range of polymers has been employed, there is a clear trend showing that with very small quantities of carbon nanotubes, it is possible to achieve the required percolation threshold. Below the percolation threshold, polymers behave as insulators for which conductivity, that increase with temperature, is generally determined by thermally assisted hopping or charge tunnelling between the charged particles [17]. On the other hand, when the percolation threshold is reached, conduction through the polymer occurs. A schematic diagram of how percolation threshold occurs is shown in **Figure 5**. Numerous studies have shown that the percolation threshold depends strongly on the polymer type, synthesis method used, aspect ratio of the CNT, how agglomerated these CNTs are in the polymer matrix and their degree of alignment [18].

http://dx.doi.org/10.5772/62508

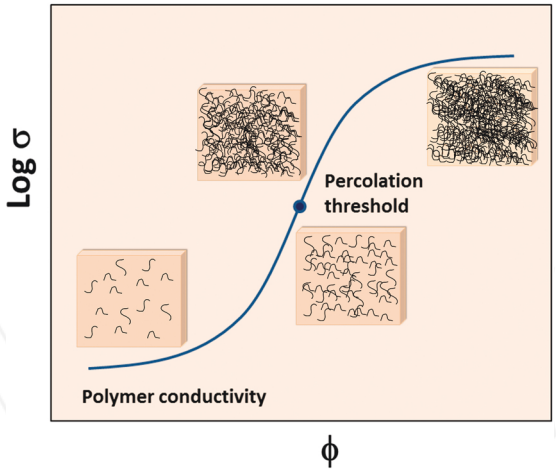

Figure 5. Schematic variation of electric conductivity with filler volume fraction for conductive nanocomposites.

The conductivity in these composites can have different values depending on the kind of conductivity that is measured. Conductivity can be measured either by direct current measurements (DC) or by alternating currents (AC). Determining the conductivity of a composite with direct current is quite straight forward, and there are several paths to achieve this. For a sample with length L and cross-section A, conductivity is given by:

$$\sigma_{DC} = \frac{L}{AR} \tag{19}$$

where R is the resistance which is measured applying a direct current and measuring a value for the voltage through the use of Ohm's Law. But this is not the only method available to calculate DC conductivity. The DC conductivity of the composites can also be determined from the frequency dependency of the AC conductivity graphs, as the value obtained for low frequencies where the conductivity is independent of the frequency used. The value of this plateau is the value of the DC conductivity. If the DC conductivity is known, then the percolation threshold can be easily calculated by using the known percolation theory, which defines an insulator-conductor transition and is stated as $\sigma_{DC}=\sigma_0(p-p_c)^t$, where σ_0 is a scaling factor, p is the CNT weight fraction, p_c is the percolation critical concentration and t is a critical exponent that governs the scaling law when close to the percolation threshold. This critical exponent is expected to depend on the system dimensionality with calculated values of 1.33 for two dimensions and a value of 2 for three dimensions [19]. The data can then be fitted to the equation in order to obtain the best-fitting values for percolation threshold and critical exponent for each case [20].

AC conductivity can be calculated as:

$$\sigma_{ac} = 2\pi f \varepsilon_0 \varepsilon^{'} \tag{20}$$

where *f* is the frequency at which the measurement is done, ε_0 is the dielectric constant in free space, $\varepsilon_r^{''}$ is the imaginary part of the complex permittivity. It is therefore obvious that this conductivity depends on the frequency used. This is the reason why DC conductivity remains as a constant value when a sweep in frequency is done, whilst AC conductivity varies. To understand fully how the changes in current affects the medium, it is important to notice that carbon nanotubes in a dielectric medium can be compared to many capacitors inside the composite.

The permittivity of a medium represents how much flux (or electric field) is generated per unit charge in the medium. More electric flux is generated in a medium with lower permittivity due to polarization effects. An efficient dielectric supports a varying charge with minimal dissipation of energy in the form of heat. The real part of the complex permittivity (ε') is related to the stored energy in the capacitor when a polarization in the dielectric occurs. It can be explained as the ability of a material to polarize as a response to an applied electric field. So, the greater the polarization developed by a material in an applied electric field, the greater the value of the dielectric constant. However, in the presence of an alternating current, this polarization is different. As the alternating current switches, the direction of the field also switches and the polarization of the dielectric needs to change in order to align with the new direction. For this new orientation to occur, a small time known as relaxation time is needed and this value is usually close to 10–11 seconds. However, if the frequency of the AC current is higher than the relaxation time, the orientation of the dipole would not be able to keep up with this change and hence will cease to contribute to the polarization of the dielectric. Therefore, as the frequency of the AC current is increased, the value of the dielectric constant drops, until it becomes equal to 1, which is the same as the dielectric constant of vacuum. Dielectrics usually loose energy through two main mechanisms and this is known as the dielectric loss parameter (ε''); in conduction loss, a flow of charge through the material causes energy dissipation, and the dielectric loss usually occurs due to the movement of the charges in an alternating magnetic field as polarization switches direction. Dielectric loss is usually highest around the relaxation or resonance frequencies of the polarization mechanisms as the polarization starts to lag behind the applied field, which causes interactions between the field and the dielectric polarization that result in heating. This must be taken into account when calculating the AC conductivity, and thus the reason why it appears in the formula mentioned above [21, 22].

5. Electromagnetic shielding of CNT composites

A wide range of values for EMI SE and conductivities have been reported in the literature over the past few decades, depending greatly on the processing method, polymer matrix and carbon nanotube type (**Table 1**). This part of the chapter is designed to be a comprehensive source for polymer composite research including fundamental relationships between the CNT structure, percolation threshold values, processing techniques, EMI SE and conductivity values. The

http://dx.doi.org/10.5772/62508

results in most cases show an enhancement of the electrical conductivity by several orders of magnitude, with the addition of CNT to the matrix.

Matrix	CNT content	Thickness (mm)	σ S/m	SET (dB)	Frequency (GHz)	Reference
PU	22 wt %	0.1	5	20	8–12	[23]
PU	10 wt% MWCNTs	>0.2	12.4	29	X-band	[24]
PU	5 wt.% SWCNTs	2	100	22	X-band	[25]
PU	10 wt% MWCNT	2.5	790	41.6	X-band	[26]
PU/PEDOT	30 wt% MWCNT	2.5	275	45	12.4	[27]
PU	76 wt%	1	2100	80	X-band	[28]
Cellulose	9.1 wt %	0.2	375	20	15–40	[29]
Cellulose	0.45 vol%	0.01–0.02	1.80	20.8	8–12	[30]
PS	15 wt%	N/A	0.1	19	8–12	[31]
PAN	2 wt%	N/A	0.006	20	0.3–3	[32]
PMMA	40 wt% MWCNT	0.06–0.165	3000	27	0.05–13.5	[33, 34]
PMMA	10 vol% MWCNT	2.1	150	40	X-band	[35]
Epoxy	15 wt% SWCNT	1.5	15	30	X-band	[36]
PC	15 wt% MWCNT	6	1000	28	X-band	[37]
PTT	10 wt% MWCNT	1.5–2	30	42	Ku-band	[38]
PVDF	3.5 wt%	1.1	100	17.7	X-band	[39]
UHMWPE	10 wt%	1	100	50	8–12.5	[40]
PEDOT	15 wt%	2.8	1935	58	12–18	[41]
HDPE	18 wt% MWCNT	3	1000	58	0.5–1.5	[42]
PE	5 wt%	2.1	80	46.4	8–12	[43]
PCL	0.25 vol%	2	2.5	80	X-band	[44]

Table 1. Electromagnetic shielding of some CNT polymer composites.

As a general trend, it can be observed that the addition of carbon nanotubes increases the conductivity and electromagnetic shielding efficiency in the composites at the same frequency value. Jia et al. [42] stated that to obtain 20 dB (the minimum commercially acceptable EMI SE), a minimum conductivity of at least 1 $S.m^{-1}$ is necessary. It is worth mentioning that the thickness of the sample is an important factor to consider [41], as thicker samples would display higher EMI SE, as shown in equation 3. According to Pande et al. [33], multiple laminated composites exhibit higher absorption capacities than bulk composites, due to internal reflections taking place between the boundaries of each layer. This effect can be compared to the effect found on Salisbury screens.

EMI SE and conductivity are affected greatly by the processing techniques used. Al-Saleh et al. [39] compares various processing techniques and concludes that the best processing method in order to obtain the best EMI SE is by melt mixing [45]. This technique is better than solution processing [12], and at the same time solution processing is better than wet mixing [39].

When good EMI SE properties are required, melt mixing is the main technique used due to several factors; first, the dispersion of the carbon nanotubes obtained with this technique is much better than the one obtained with other techniques. Secondly, the nanotubes do not break with melt mixing, unlike with techniques such as ball milling or co-precipitation, which gives the composite a better conductivity overall and therefore enhances the electromagnetic shielding properties. Ultimately, melt mixing does not use any solvents, making this technique environmental-friendly unlike in-situ polymerization or solvent casting [46].

Some studies have shown that the percolation threshold depends strongly on the alignment and aspect ratio of the filler used. On this regard, rod-like fillers such as carbon nanotubes exhibit higher aspect ratios than spherical particles, allowing the percolation threshold to be achieved with lower filler concentration. If the fillers stick together, in a process known as agglomeration, the percolation threshold rises due to the aspect ratio being smaller as compared to well-dispersed fillers. Again, continuing with the importance of aspect ratio, Gupta et al. [26] and Huang et al. [35] demonstrated that the longer the CNTs the better the conductivity and therefore the electromagnetic shielding efficiency. Qin et al. [10] and Du et al. [18] proved that a secondary mechanism affecting the percolation threshold exists: alignment percolation. It was shown that aligned fillers tend to have higher percolation thresholds than anisotropic oriented fillers. This is due to the probability of a conductive path forming in the matrix being higher, than in oriented filler composites. Also, aligned fillers have worse conductivity, as fewer contacts between the tubes exist [45].

The type of carbon nanotube used, being single-walled carbon nanotubes (SWCNT) and multi-walled carbon nanotubes (MWCNT) the main types, also seems to have an effect on the EMI SE parameters. Comparing SWCNTs to MWCNTs, it is possible to notice the greater number of defects present in the MWCNT, which also causes higher permittivity. In a series of papers, it has been studied that the defects and impurities of CNTs have become impediment to properly describe the polarization mechanisms and ohmic losses of the composite materials [41]. This makes MWCNT have higher EMI SE, with the main shielding mechanism being absorption. However, other references analyse the differences in conductivity caused by the type of CNT used, and it seems that the impact on conductivity depending on CNT type is very small [42].

It is widely accepted that altering the carbon nanotube structure by functionalizing them disrupts the conductivity of isolated nanotubes. However, there are exceptions to this rule, as demonstrated by Tamburri et al. (2005) [22] where functionalizing the SWCNT with carboxylic groups enhanced the conductivity in the composites by a factor of 140, as compared with the unfunctionalized nanotubes which only showed an increase of 20 times the conductivity. This functionalization also improved the dispersion in the matrix, outweighing the advantages as compared to untreated carbon nanotubes. Apart from good EMI SE, composites must fulfil some important requirements, such as enhanced mechanical properties [27], light weight [40],

http://dx.doi.org/10.5772/62508

good processability [23–26], low cost [38] and environmental-friendly [29, 44]. This is the reason why several polymer matrices have been studied in order to suit each and any of the desired applications, in particular EMI SE.

Dielectric properties of the polymer used are important, as polymers with high permittivity result in higher conductivities. The main objective is to search for conductive polymers (such as PEDOT), in order to block the EM radiation. However, some polymers are not conductive and alternatives for achieving high conductivities are searched. There are two main categories of the polymers used to achieve conductive composites: intrinsically conductive polymers (ICPs) and polymer composites with conductive particles. Polypyrrole and polyaniline are the most frequently used ICPs. Non-conductive polymers have been added to these composites to enhance the mechanical integrity of the mixture, as ICPs are normally brittle. Farukh et al. [27] used polyurethane with the previously mentioned PEDOT, with the objective to obtain a final composite with better elasticity, high impact strength and elongation properties. The drawback in most cases is the high load of ICP that is needed to attain high conductivities, which is detrimental for the processability of the blends. The alternative like mentioned above is to insert conductive fillers in the polymer matrix. The fillers do not depend only on the intrinsic electrical properties of the individual particles but also depend on the interparticle interactions. On this regard, carbonaceous materials such as CNTs and graphene have been used as conductive fillers, as they possess large conductivities with very low densities as compared to metallic particles, providing the composite with very good electrical properties and maintaining low weights.

From a theoretical point of view, four composites with a thickness of 4 mm and varying CNT compositions, which can originate DC conductivities of 20, 30, 40 and 50 $S.m^{-1}$, are studied. If the reflection and absorption shielding are calculated (**Figure 6**), it will be observed that increasing the conductivity increases both shielding mechanisms.

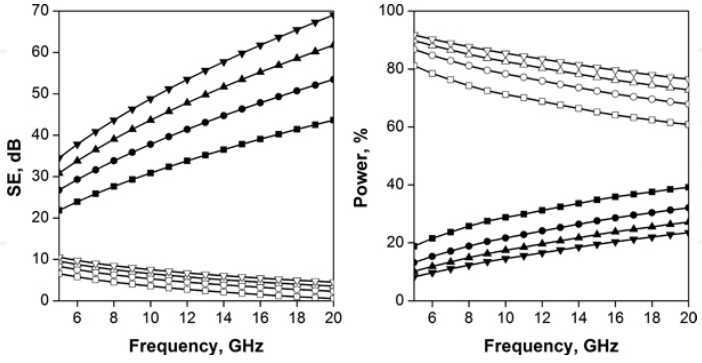

Figure 6. Reflection shielding and reflection coefficient (R) of specimens with 20 (□), 30 (○), 40 (Δ) and 50 $S.m^{-1}$ (▽). Absorption shielding and transmission coefficient through the first plane of incidence ($1 - R$) of specimens with 20 (■), 30 (●), 40 (▲) and 50 (▼) $S.m^{-1}$.

The absorption shielding is the preferred mechanism in all cases with values higher than 20 dB for samples with only 4 mm thickness, whereas the reflection is always less than 10 dB. This would suggest that the predominant process is absorption. However, if the reflection coefficient from equation 8 is calculated, the conclusions are not the same.

Figure 6 shows the reflection coefficient (R) and the transmission coefficient through the first plane of incidence ($1 - R$). If these values are analysed, it is observed that between 60 and 90% of the incident radiation is reflected, while the transmission coefficient is never over 40%. This means that while the preferred shielding mechanism is the absorption, most of the radiation will not be able to enter the material and therefore will be unable to absorb it.

We can conclude, from the previous explanation, that both reflection and absorption increase with the conductivity of the material. High conductivity promotes both processes: absorption increases but reflection is also favoured, so that just a small part of radiation is able to penetrate into the material and behaves as a reflector. Low conductivity worsens both reflection but mainly absorption, as more radiation is able to penetrate into the material and thus be absorbed. Nevertheless, when conductivity is low, the multiple reflection process increases and the material behaves as a reflector. Therefore, is high or low conductivity necessary? "That is the question".

Reflection process is located in the incidence plane, while absorption process depends on the material thickness. Modification of the first incidence plane to decrease the impedance mismatch between the medium and the material is therefore necessary.

In an attempt to minimize the reflection from a surface, it is useful to consider the physical equations that represent the reflection process. This equation describes the reflection coefficient at an interface:

$$r = \frac{\eta_M - \eta_o}{\eta_M + \eta_o} = \frac{Z_M - Z_o}{Z_M + Z_o} \tag{22}$$

where r is the reflection coefficient and η the admittance of the propagating medium (subscript o for incident medium or air and M for the substrate). The admittance in this equation can be replaced by the intrinsic impedance ($Z = 1/\eta$). The reflection coefficient falls to zero when $\eta_M = \eta_o$, or in other words the material in the layer is impedance matched to the incident medium.

Absorbers can be classified into impedance matching and resonant absorbers (Salisbury screens). Impedance matching (pyramidal) absorbers are shielding materials that reduce the impedance step between the incident and the absorbing media. In resonant materials, the impedance is not matched between incident and absorbing media and the material is thin so that the power is not completely absorbed. Pyramidal absorbers [45] are typically thick materials with pyramidal or cone structures extending perpendicular to the surface in a regularly spaced pattern. The interface of these structures presents a gradual transition in impedance from air to that of the absorber. The height and periodicity of the pyramids tend

http://dx.doi.org/10.5772/62508

to be on the order of one wavelength. The disadvantage of pyramidal absorbers is their thickness and fragility. They are usually used for anechoic chambers.

It is well known that a "Salisbury screen" is based on a sandwich structure of a dielectric between two conductive sheets. When the electromagnetic wave is incident upon the first layer, a portion of the radiation is reflected, while another portion penetrates into the dielectric sheet towards the second conductive sheet. In the second plane of incidence, the reflection of radiation occurs in the direction of the first plane of incidence and part of this is able to go through this conductive sheet and towards the exterior. The reflected radiation in the first and the second planes can produce constructive and destructive interference. Destructive interference occurs when the distance between the conductive sheets is a multiple of a quarter of the wavelength (see **Figure 7**).

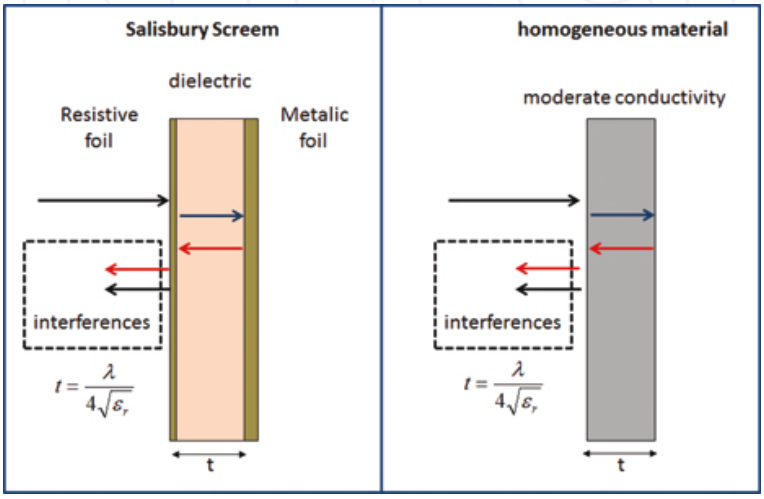

Figure 7. Interferences between reflections produced over the first and second planes in a Salisbury screen and a homogeneous conductive material.

The process is equivalent in homogeneous material with moderate conductivity. In both cases, a maximum electromagnetic shielding occurs at a certain frequency. In **Figure 7**, a qualitative behaviour of (SE) with the permittivity in samples with thickness of 4 mm is shown. It is possible to observe how a maximum displacement of the shielding occurs by increasing the permittivity of the dielectric. In homogeneous materials with moderate conductivity, processes of energy dissipation can exist. These processes that arise from the first to the second plane, back and forth propagation of the waves, dissipate some of the radiation and therefore interferences that should have been produced in the first plane are lower.

Another form to minimize the impedance mismatch between the medium and the sample is the use of porous materials. To address the problem of the impedance mismatch when using highly conductive carbonaceous nanoparticles, special focus on their microscopic organization

should be taken. Optimally, a highly porous outer surface with a pore size similar to the incident radiation would be required. In principle, when radiation impinges on the surface of a porous conductive material, it becomes distributed among the pores and their walls. The major portion of the reflected radiation will arise from reflections with the pore walls, being reflections from the inner part of the pores a much smaller contribution. Therefore, the fraction and size of the pores created on the surface of a conductive compound may be good tools for modulating the phenomenon of electromagnetic reflection. If the process of reflection is decreased, a larger fraction of the radiation will penetrate into the material, being able to remove it by another mechanism (absorption). Different studies support this effect. For example, Zhao et al. [47] studied the shielding behaviour of carbon fibre epoxy composites, varying the thickness of the fibres and the size of the grid; the authors observed that when the ratio grid size/thickness of fibre increased, the reflection of electromagnetic radiation decreased. These data confirm the possibility to decrease the impedances mismatch for minimizing the reflection losses using porous structures in such a way that the walls are formed by conductive fibres for increasing the absorption in the material.

An important consideration for the designer of absorbing materials concerns the absorption efficiency with respect to weight. CNTs absorbing properties originate either from polarization, ohmic losses or multiple scattering due to the large specific surface area. There are differences in absorbing properties depending on the type of CNTs [48]. As we have commented previously, compared with single-walled CNTs (SWCNTs), multi-walled CNTs (MWCNTs) have more defects due to their complicated structure and higher permittivity, and their absorption is due to dielectric relaxation. The absorption properties of CNT composites depend on multiple factors [4, 10]: interfacial polarization, particle geometry, fibre concentration and particle dispersion.

Composite materials with conducting fibres have a frequency-dependent effective permittivity. To characterize the electromagnetic properties of composite media, it is important to know the electromagnetic parameters of a host (matrix, base) material and inclusions.

6. Trend in electromagnetic shielding materials

The development of new materials with the purpose of electromagnetic shielding has evolved in the past few years towards the study of carbon structures. The three principal types of carbon architectures employed for this purpose are carbon nanotubes and graphene.

6.1. Carbon nanotubes

Carbon nanotubes, in the form of cylindrical carbon molecules, exhibit high strength and count also with high electrical and thermal conductivity due to their symmetry. These allotropes can be formed by a single (SWNT) or several walls (MWNT), and the variation in their diameter can vary greatly their electrical properties [46, 49]. As studied in previous sections, their aspect ratio has a great effect in electromagnetic shielding applications. Carbon nanotubes have been used in several investigations as reinforcements in host matrices, in order to accomplish a 3D

http://dx.doi.org/10.5772/62508

shielding structure. In particular, Li et al. merged single-walled carbon nanotubes with a polymeric matrix (15%), and a EMI SE of 15–20 dB was obtained for 1.5 GHz of frequency, a frequency range dominated by reflection [50]. Increasing their weight percentage in the composite enhances the shielding efficiency of the material but decreases its mechanical properties and processability, so a compromise between these properties for each application must be obtained. **Figure 8** shows CNT foams synthesized by chemical vapour deposition (CVD) with SE_T of to 22 dB in almost the entire frequency window (1–18 GHz) for the 2.38 mm thick CNT-foam slab [11]. CNT foams possess extremely low densities lower than 0.02 g·cm^{-3} and the higher specific shielding efficiency obtained of 1100 dB·cm^3·g^{-1}.

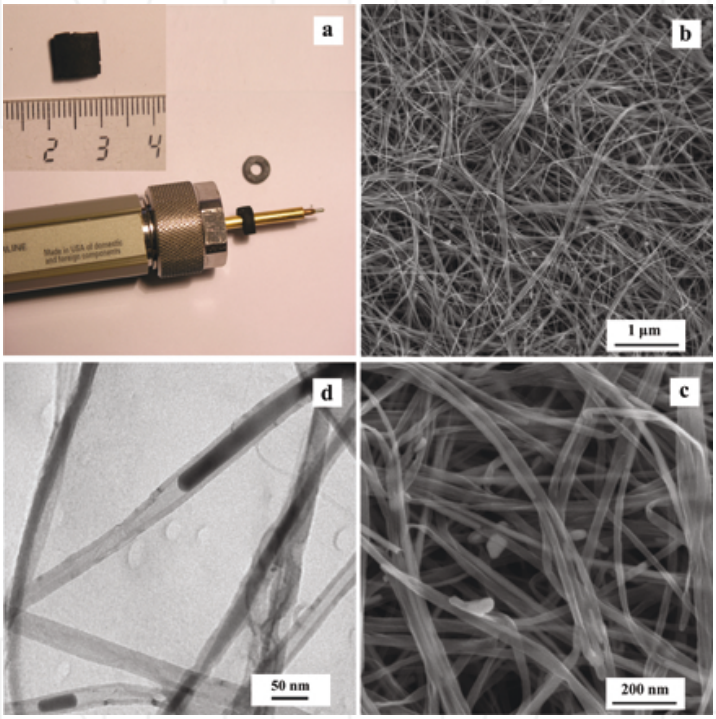

Figure 8. (a) Specimens and coaxial airline used for EMI shielding measurements. (b,c) SEM images of sponges. (d) TEM image of CNTs that are forming the sponges [13].

6.2. Graphene

Graphene can be regarded as the current state-of-the-art material in the study of EMI shielding. It is a two-dimensional hexagonally-packed carbon structure, of sp^2 hybridization, where the free carbon electrons align perpendicular to the plane, thus forming an out-of-plane π bond. Graphene counts with high mechanical properties, charge carriers mobility, thermal conductivity and light weight and quantum Hall effect at room temperature. Its ability to form three-

dimensional structures is the main advantage that differentiates it from carbon fibres and nanotubes, enhancing this carbon hybrid as a suitable candidate for the ES of structures, such as radars.

Conductivity of graphene decreases as the layer increases, approaching to that of graphite. This conductivity is determinant for the losses in reflection and conduction; on the other hand, polarization loss is enhanced by the functional groups and defects. The decreased thickness of graphene enhances the conduction loss due to the increase in conductive paths. Polarization loss is the reason why chemically fabricated graphene is normally used for EMI shielding, whose conductivity is, in fact, lower.

Over time, ultra-thin graphene composites arose, with which more than 20 dB of EMI SE could be achieved. This mixture combines the excellent EMI shielding properties of graphene, with the mechanical strength of the matrix material. Graphene has been blended with multiple polymers, such as epoxy [51], polystyrene (PS) [52], polyethylene (PE) [53] and polyurethane (PU) [54, 55], among others [56].

More specifically, as mentioned before, the possibility to form three-dimensional (3D) porous foams with it have been carefully studied in recent investigations. As porous carbon structures, they count with excellent conductivity, and a high specific surface area can be achieved. With these holes, reflection can be lowered, due to the decrease in the external surface of the structure, and absorption can be enhanced, thanks to the multi-reflection inside the pores. **Figure 6** shows a pore structure inside a three-dimensional CNT structure.

In an investigation of Zhang et al. [57], a three-dimensional graphene porous structure was fabricated by hydrothermal polymerization of a carbon source (a mixture of phenol and formaldehyde) with GO (graphene oxide) in order to get these three-dimensional structures, which were later activated chemically—with KOH—to achieve the conductivity and desired surface specific area values. It is worth mentioning that surface specific area increases when GO is combined with a carbon source: the carbon source or GO by themselves had much lower values of specific surface area. The obtained material, few-nanometres long, had a specific surface area of 3523 $m^2 \cdot g^{-1}$ and a conductivity of 303 $S.m^{-1}$.

Another type of graphene three-dimensional structures were the graphene sponge (GS) scaffolds infiltrated in epoxy resin to form a GS/epoxy composite, built and studied by Li et al. [58]. There are two main problems of manufacturing graphene-polymer composites. The first is the reduced dispersion of graphene in a polymeric matrix, as a result of the graphene sheets' strong intermolecular connections and their high specific surface area; the second one arises when low filler content is added, so that the graphene sheets are surrounded by polymer chains, which affects the thermal and electrical conductivity of the composite material. It is clear then that an optimum ratio of polymer/graphene is needed in order to avoid these problems. In this study, the assembly into a three-dimensional sponge of GO sheets was performed using a hydrothermal plus freeze-drying treatment, followed by a vacuum infusion process to obtain the final composite. This method permits ease in the production, saving resources (low cost) and can be applied at different scales.

http://dx.doi.org/10.5772/62508

GO suspension was synthesized using the modified Hummers' approach. The GS obtained had a density of 0.022 $g.cm^{-3}$, an ultra-low value for this property. The epoxy resin could be infused into the GS because of its open pore structure. The size and of the GS did not change after the vacuum process, showing that no shrinkage occurs. It could be stated that the conductivity of the GS/epoxy composite was comparable to that of the GS. It is worth to mention that the conductivity of the graphene sponges is isotropic; an effect accredited to the random distribution of the reduced graphene sheets.

The thickness of these graphene structures is also of vital importance for the electromagnetic shielding efficiency. Song et al. [59] proved in their investigation that the SE of graphene-based structures increased with increasing thickness of the sponges: 28 dB for 2mm and 36 dB for 3 mm of thickness.

6.3. Graphene-CNT hybrid structures

In recent investigations, the possibility to blend large surface area, one-dimensional carbon nanotubes within a high charge density, two-dimensional graphene matrix has been studied. Generally, CNTs tend to agglomerate in organic dispersion; therefore, numerous efforts were developed to disperse the CNT by using micelles, ionic liquids, surfactants, polymer wrapping and other chemical functionalization approaches. It has been proved that GO could be a better dispersant to form a stable dispersion of CNT and the resulted dispersion is a novel hybrid named as graphene oxide-CNT (GO-CNT) [60]. Studies proved that GO-CNT and graphene-CNT hybrid nanomaterials exhibit higher electrical conductivities, large specific area and catalytic properties compared with either pristine CNTs or GO/graphene [61]. The strong π–π stacking interaction operating between graphene and CNT makes a three-dimensional network for the hybrid material and provide exceptional stability [62]. The CNTs act as conducting wires inside the already conducting graphene structure, thus promoting the conductivity of the hybrid material. In particular, Mani et al. [63] compared the suitability of graphene oxide (GO) structures merged with CNTs. GO was obtained by chemical oxidation of graphite into graphite oxide, and subsequent exfoliation into monolayer graphene. It could be stated that GO was more beneficial to obtain a stable dispersion of CNTs in its three-dimensional structure. The forces between these two architectures were found to be π-π interactions. In another study, Chen et al. [64] used graphene-MMCNTs structures to study the EMI shielding of these hybrid structures. A shield of 80-90% of the power density could be achieved with these sponges.

7. Conclusions

The latest techniques and strategies to develop new CNT/polymer composites with electromagnetic shielding properties have been reviewed. In composites with CNTs dispersed into a polymeric matrix, better EMI SE results are obtained with the increase of sample thickness and filler conductivity. Thus, it is possible to conclude that multi-walled carbon nanotubes exhibit better shielding properties than single-walled carbon nanotubes. At the same time,

having longer or better dispersed carbon nanotubes translates into lower volume fractions of filler needed in order to reach the percolation threshold in the composite. At the same time, the possibility of minimizing the reflection mechanisms in electromagnetic shielding leading to purely (or mostly) absorbent materials has been proved. Equilibrium between the morphology and the conductivity of the material must be searched, being this one of the reasons why foams are gathering most of the attention in the field, as they allow the radiation to enter through the porous surface and is then absorbed in the interior. At the same time, it possesses the enormous advantages of being light-weight and easy to manufacture, opening the field of these foams for new application. A theoretical introduction to the problem of electromagnetic shielding has been introduced, showing an insight into the ways to calculate it and the measuring equipment used at present for this purpose.

Acknowledgements

This work was supported by the grant Nanoarq (MAT2014-57557-R) from the Spanish Ministerio de Ciencia e Inovación.

Author details

Marta González, Guillermo Mokry, María de Nicolás, Juan Baselga and Javier Pozuelo*

*Address all correspondence to: jpozue@ing.uc3m.es

Materials Science and Engineering and Chemical Engineering (IAAB), Carlos III University of Madrid, Spain

References

[1] Christopoulos C. Principles and Techniques of Electromagnetic Compatibility. CRC Press; 2007, 1–4.

[2] Clayton R.P. Frontmatter. In: Introduction to Electromagnetic Compatibility. 2nd ed. Hoboken, NJ: John Wiley & Sons, Inc.; 2005, 1–48.

[3] Tong X.C. Advanced Materials and Design for Electromagnetic Interference Shielding. CRC Press; 2008, 1–35.

[4] Yusoff A.N., Abdullah M.H., Ahmad S.H., Jusoh S.F., Mansor A.A., Hamid S.A.A. Electromagnetic and absorption properties of some microwave absorbers. J. Appl. Phys. 2002;92:876.

[5] Chung D.D.L. Electromagnetic interference shielding effectiveness of carbon materials. Carbon 2001;39:279–285.

[6] Huang J.C. EMI shielding plastics: A review. Adv. Polym. Technol. 1995;14:137–150.

[7] Das N.C., Khastgir D., Chaki T.K., Chakraborty A. Electromagnetic interference shielding effectiveness of carbon black and carbon fibre filled EVA and NR based composites. Compos. Part A Appl. Sci. Manuf. 2000;31:1069–1081.

[8] Vovchenko L., Perets Y., Ovsienko I., Matzui L., Oliynyk V., Launetz V. Shielding coatings based on carbon–polymer composites. Surf. Coatings Technol. 2012;211:196–199.

[9] Ren F., Yu H., Wang L., Saleem M., Tiana Z., Rena P. Current progress on the modification of carbon nanotubes and their application in electromagnetic wave absorption. RSC Adv. 2014;4:14419–14431.

[10] Qin F., Brosseau C. A review and analysis of microwave absorption in polymer composites filled with carbonaceous particles. J. Appl. Phys. 2012;111:061301.

[11] Gonschorek K.H., Vick R. Electromagnetic Compatibility for Device Design and System Integration, Chap. 17: Skin Effect and Shielding Theory of Schelkunoff. Berlin, Heidelberg: Springer; 2009, 377–392.

[12] Al-Saleh M.H., Sadaah W.H., Sundararaj U. EMI shielding effectiveness of carbon based nanostructured polymeric materials: a comparative study. Carbon 2013;60:146–156.

[13] Crespo M., González M., Elías A.L., Rajukumar L.P., Baselga J., Terrones M., Pozuelo J. Ultra-light carbon nanotube sponge as an efficient electromagnetic shielding material in the GHz range. Phys. Status Solidi RRL 2014;8:698–704.

[14] Zois H., Apekis L., OmastováM. Electrical properties of carbon black-filled polymer composites. Macromol. Symposia 2001;170:249–256.

[15] Ezquerra T.A., Connor M.T., Roy S., Kulescza M., Fernandes-Nascimento J., Baltá-Calleja F.J. Alternating-current electrical properties of graphite, carbon-black and carbon-fiber polymeric composites. Compos. Sci. Technol. 2001;61:903–909.

[16] Kortschot M., Woodhams R. Computer simulation of the electrical conductivity of polymer composites containing metallic fillers. Poly. Compos. 1988;9:60–71.

[17] Barrau S., Demont P., Peigney A., Laurent C., Lacabanne C. DC and AC conductivity of carbon nanotubes−polyepoxy composites. Macromolecules 2003;36:5187–5194.

[18] Du F., Fischer J.E., Winey K.I. Effect of nanotube alignment on percolation conductivity in carbon nanotube/polymer composites. Phys. Rev. B Condens. Matter Mater. Phys. 2005;72:1–4.

[19] Stauffer D., Aharony A. Introduction to Percolation Theory. CRC Press; 1994; pp. 1–92.

[20] Bauhofer W., Kovacs J.Z. A review and analysis of electrical percolation in carbon nanotube polymer composites. Compos. Sci. Technol. 2009;69: 1486–1498.

[21] Du J., Hsieh Y.L. Cellulose/chitosan hybrid nanofibers from electrospinning of their ester derivatives. Cellulose 2009;16:247–260.

[22] Tamburri E., Orlanducci S., Terranova M.L., Valentini F., Palleschi G., Curulli A., Brunetti F., Passeri D., Alippi A., Rossi M. Modulation of electrical properties in single-walled carbon nanotube/conducting polymer composites. Carbon 2005;43:1213–1221.

[23] Hoang A.S. Electrical conductivity and electromagnetic interference shielding characteristics of multiwalled carbon nanotube filled polyurethane composite films. Adv. Nat. Sci. Nanosci. Nanotechnol. 2011;2:025007/025001-025007/025005.

[24] Gupta T.K., Singh B.P., Dhakate S.R., Singh V.N., Mathur R.B. Improved nanoindentation and microwave shielding properties of modified MWCNT reinforced polyurethane composites. J. Mat. Chem. A 2013;1:78.

[25] Liu Z., Bai G., Huang Y., Li F., Ma Y., Guo T., He X., Lin X., Gao H., Chen Y. Microwave absorption of single-walled carbon nanotubes/soluble cross-linked polyurethane composites. J. Phys. Chem. C 2007;111:13696.

[26] Gupta T.K., Singh B.P., Teotia S., Katyal V., Dhakate S.R., Mathur R.B. Designing of multiwalled carbon nanotubes reinforced polyurethane composites as electromagnetic interference shielding materials. J. Polym. Res. 2013;20:169.

[27] Farukh M., Dhawan R., Singh B.P., Dhawan S.K. Sandwich composites of polyurethane reinforced with poly(3,4-ethylene dioxythiophene) coated multiwalled carbon nanotubes with exceptional electromagnetic interference shielding properties. RSC Adv. 2015;5:75229–75238.

[28] Zeng Z., Chen M., Jin H., Li W., Xue X., Zhou L., Pei Y., Zhang H., Zhang Z. Thin and flexible multi-walled carbon nanotube/waterborne polyurethane composites with high-performance electromagnetic interference shielding. Carbon 2016;96:768–777.

[29] Imai M., Akiyama K., Tanaka T., Sano E. Highly strong and conductive carbon nanotube/cellulose composite paper. Compos. Sci. Technol. 2010;70:1564–1570.

[30] Yang Y., Gupta M.C., Dudley K.L., Lawrence R.W. Conductive carbon nanofiber-polymer foam structures. J. Nanosci. Nanotechnol. 2005;5:927–931.

[31] Chen I.H., Wang C.C., Chen C.Y. Fabrication and structural characterization of polyacrylonitrile and carbon nanofibers containing plasma-modified carbon nanotubes by electrospinning. J. Phys. Chem. C 2010;114:23532–13539.

[32] Kim H.M., Kim K., Lee C.Y., Joo J., Cho S.J., Yoon H.S., Pejakovic D.A., Yoo J.W., Epstein A.J. Electrical conductivity and electromagnetic interference shielding of multiwalled carbon nanotube composites containing Fe catalyst. J. Appl. Phys. Lett. 2004;84:589.

[33] Pande S., Singh B.P., Mathur R.B., Dhami T.L., Saini P., Dhawan S.K. Improved electromagnetic interference shielding properties of MWCNT–PMMA composites using layered Structures. Nanoscale Res. Lett. 2009;4:327.

[34] Kim H.M., Kim K., Lee S.J., Joo J., Yoon H.S., Cho S.J., Lyu S.C., Lee C.J. Charge transport properties of composites of multiwalled carbon nanotube with metal catalyst and polymer: application to electromagnetic interference shielding. Curr. Appl. Phys. 2004;4:577–580.

[35] Huang Y., Du F., He X., Lin X., Gao H., Ma Y., Li F., Chen Y., Eklund P.C. Electromagnetic interference (EMI) shielding of single-walled carbon nanotube epoxy composites. Nano Lett. 2006;6:1141.

[36] Singh A.P., Gupta B.K., Mishra M., Govind M., Chandra A., Mathur R.B., Dhawan S.K. Multiwalled carbon nanotube/cement composites with exceptional electromagnetic interference shielding properties. Carbon 2013;56:455.

[37] Gupta A., Choudhary V. Electromagnetic interference shielding behaviour of poly(trimethylene terephthalate)/multi-walled carbon nanotube composites. Compos. Sci. Technol. 2011;71:1563–1568.

[38] Arjmand M., Sundararaj U. Electromagnetic interference shielding of nitrogen-doped and undoped carbon nanotube/polyvinylidene fluoride nanocomposites: a comparative study. Compos. Sci. Technol. 2015;118:257–263.

[39] Al-Saleh M.H. Influence of conductive network structure on the EMI shielding and electrical percolation of carbon nanotube/polymer nanocomposites. Synth. Metals 2015;205:78–84.

[40] Farukh M., Singh A.P., Dhawan S.K. Enhanced electromagnetic shielding behavior of multi-walled carbon nanotube entrenched poly (3,4-ethylenedioxythiophene) nanocomposites. Compos. Sci. Technol. 2015;114:94–102.

[41] Yim Y.J., Park S.J. Electromagnetic interference shielding effectiveness of high-density polyethylene composites reinforced with multi-walled carbon nanotubes. J. Indus. Eng. Chem. 2015;21:155–157.

[42] Jia L.C., Yan D.X., Cui C.H., Jiang X., Ji X., Li Z.M. Electrically conductive and electromagnetic interference shielding of polyethylene composites with dev carbon nanotube networks. J. Mater. Chem. C 2015;00:1–8.

[43] Huang H.D., Liu C.Y., Zhou D., Jiang X., Zhong G.J., Yan D.Y., Li Z.M. Cellulose composite aerogel for highly efficient electromagnetic interference shielding. J. Mater. Chem. A 2015;3:4983–4991.

[44] Thomassin J.M., Pagnoulle C., Bednarz L., Huynen I., Jerome R., Detrembleur C. Foams of polycaprolactone/MWNT nanocomposites for efficient EMI reduction. J. Mater Chem. 2008;18:792–796.

[45] Arjmand M., Apperley T., Okoniewski M., Sundararaj U. Comparative study of electromagnetic interference shielding properties of injection molded versus compression molded multi-walled carbon nanotubes/polystyrene composites. Carbon 2012;50(14):5126–5134.

[46] Thomassin J.M., Jérôme C., Pardoen T., Bailly C., Huynen I., Detrembleur C. Polymer/carbon based composites as electromagnetic interference (EMI) shielding materials. Mater. Sci. Eng. R Rep. 2013;74:211–232.

[47] Zhao N., Zou T., Shi C., Li J., Guo W. Microwave absorbing properties of activated carbon-fiber felt screens (vertical-arranged carbon)/epoxy resin composites. Mater. Sci. Eng. B. 2006;127:207–211.

[48] Al-Saleh M.H., Sundararaj U. Electromagnetic interference shielding mechanisms of CNT/polymer composites. Carbon 2009;47:1738–1746.

[49] Celozzi S., Araneo R., Lovat G. Electromagnetic Shielding. IEEE Press; 2008.

[50] Li N., Huang Y., Du F., He X., Lin X., Gao H., Ma L.F., Chen Y., Eklund P.C. Electromagnetic interference (EMI) shielding of single-walled carbon nanotube epoxy composites. Nano Lett. 2006;6(6):1141–1145.

[51] Jiang J.J., Wang Y., Liang J.J., Wang Y., Huang Y., Ma Y.F., Liu Z.F., Cai J.M., Zhang C.D., Gao H.J., Chen Y.S. Electromagnetic interference shielding of graphene/epoxy composites. Carbon 2009;47:922–925.

[52] Yan D.X., Pang H., Li B., Vajtai R., Xu L., Ren P.G., Wuang J.H., Li Z.M. Structured reduced graphene oxide/polymer composites for ultra-efficient electromagnetic interference shielding. Adv. Funct. Mater. 2015;25:559–566.

[53] Yan D.X., Pang H., Xu L., Bao Y., Ren P.G., Lei J., Li Z.M. Electromagnetic interference shielding of segregated polymer composite with an ultralow loading of *in situ* thermally reduced graphene oxide. Nanotechnology 2014;25:145705.

[54] Hsiao S.T., Ma C.C.M., Tien H.W., Liao W.H., Wang Y.S., Li S.M., Huang Y.C. Using a non-covalent modification to prepare a high electromagnetic interference shielding performance graphene nanosheet/water-borne polyurethane composite. Carbon 2013;60:57–66.

[55] Hsiao T., Ma C.C.M., Tien H.W., Liao W.H., Wang Y.S., Li S.M., Yang C.Y., Lin S.C., Yang R.B. Effect of covalent modification of graphene nanosheets on the electrical property and electromagnetic interference shielding performance of a water-borne polyurethane composite. Acs. Appl. Mater. Inter. 2015;7:2817–2826.

[56] Chen Z.P., Xu C., Ma C.Q., Ren W.C., Cheng H.M. Lightweight and flexible graphene foam composites for high-performance electromagnetic interference shielding. Adv. Mater. 2013;25:1296–1300.

[57] Zhang L., Zhang F., Yang X., Long G., Wu Y., Zhang T., Leng K., Huang Y., Ma Y., Yu A., Chen Y. Porous 3D graphene-based bulk materials with exceptional high surface area and excellent conductivity for supercapacitors. Sci. Rep. 2013;3:1408.

[58] Li Y., Samad Y.A., Polychronopoulou K., Alhassan S.M., Liao K. Highly electrically conductive nanocomposites based on polymer-infused graphene sponges. Sci. Rep. 2014;4:4652.

[59] Song W.L., Guan X.T., Fan L.Z., Cao W.Q., Wang C.Y., Cao M.S. Tuning three-dimensional textures with graphene aerogels for ultra-light flexible graphene/texture composites of effective electromagnetic shielding. Carbon 2015;93:151–160.

[60] Cao M.S., Wang X.X., Cao W.Q., Yuan J. Ultrathin graphene: electrical properties and highly efficient electromagnetic interference shielding. J. Mat. Chem. C 2015;3:6589–6599.

[61] Mani V., Chen S.M., Lou B.S. Three dimensional graphene oxide-carbon nanotubes and graphene- carbon nanotubes hybrids. Int. J. Electrochem. Sci. 2013;2013:11641–11660.

[62] Kachoosangi R.T., Musameh M.M., Abu-Yousef I. Carbon nanotube-ionic liquid composite sensors and biosensors. Anal Chem. 2009;81(1):435–442.

[63] Mani V., Devadas B., Chen S.M. Direct electrochemistry of glucose oxidase at electrochemically reduced graphene oxide-multiwalled carbon nanotubes hybrid material modified electrode for glucose biosensor. Biosens. Bioelectron. 2013;41:309–315.

[64] Chen Y.J., Li Y., Chu B.T.T., Kuo I.T., Yip M., Tai N. Porous composited coated with hybrid nano carbon materials perform excellent electromagnetic interference shielding. Composit. B 2015;70:231–237.